MAGNETOHYDRODYNAMICS Vol. 51 (2015), No. 2, pp. 203–213

INSTABILITY OF ELECTROLYTE FLOW DRIVEN BY AN AZIMUTHAL LORENTZ FORCE

J. Pérez-Barrera[1], *J.E. Pérez-Espinoza*[1], *A. Ortiz*[1,2]
E. Ramos[1], *S. Cuevas*[1]

[1] *Instituto de Energías Renovables, Universidad Nacional Autónoma de México, Temixco, Morelos, 62580 MEXICO*
[2] *Universidad Autónoma de Baja California, Blvd. Benito Juárez S/N. Unidad Universitaria, Mexicali, B.C. 21280 MEXICO*

We describe of an instability in a free surface flow produced by an azimuthal Lorentz force in a layer of an electrolyte contained in an open electromagnetic stirrer with cylindrical geometry. The force is created by the interaction of an applied radial electric current within the range 25–400 mA and an approximately constant magnetic field (0.04 T) parallel to the cylinder's axis. The flow instability leads to the formation of cyclonic vortices close to the internal electrode and anticyclonic vortices close to the external electrode, in the plane normal to the magnetic field. Flow visualization using dye reveals that the travelling anticyclonic vortices remain for long times once they appear. Detailed flow patterns are explored through Particle Image Velocimetry measurements with the aim of clarifying the mechanisms that originate the vortex formation.

Introduction. Magnetohydrodynamic flows in annular ducts have been widely explored both experimentally and theoretically. From the experimental point of view, annular ducts avoid the difficulty of considering the entrance region that is present in rectilinear ducts under a strong uniform magnetic field. In the most common configuration, the annular duct is formed in the gap between two coaxial electrically conducting cylinders, limited by insulating top and bottom walls. By placing the duct at the center of a magnetic solenoid, an approximately uniform magnetic field parallel to the cylinder's axis is induced. If an electric potential difference is applied between the coaxial cylinders, a radial electric current density will arise in the conducting fluid. The interaction of the radial current with the axial magnetic field produces an azimuthal Lorentz force that drives the flow. Some early works dealt with this problem theoretically and analytical solutions for simplified models were obtained [1–3]. Since the pioneering works of Baylis [4] and Baylis and Hunt [5], attention has been mainly focused on liquid metal flows at high Hartmann numbers, motivated by important applications related to metallurgy and fusion blanket technologies. Experimental investigations in a different configuration with ring-shaped electrodes in the bottom wall showed the appearance of instabilities and even turbulence in liquid metal flows with free shear layers [6, 7]. Moresco and Alboussière [8] used the annular duct configuration to investigate experimentally the stability properties of the Hartmann layer and the transition to turbulence in liquid metal flow. In turn, Mikhailovich [9] performed an experimental study of the rotaing flow of liquid metal driven by an azimuthal force in an annular container. This author analyzed the behavior of mean and fluctuating values of the azimuthal velocity component in different conditions and found that the mean values of this component differed from the known analytical solutions. In a more recent study, Mikhailovich *et al.* [10] analyzed the decay of mean velocity components and turbulent fluctuations, as well as the peculiarities of spectral characteristics of such flows. Zhao *et al.* [11] explored numerically the centrifugal instability between coaxial infinite conducting cylinders at large Hartmann numbers, disregarding the Hartmann walls with the aim to understand better the role of the sidewall layers. In a subsequent numerical study, Zhao and Zikanov [12] considered the existence of insulating top and bottom Hartmann walls in an annular (toroidal) duct of square cross-section with the same geometry and parameter range used in the experiment by Moresco and Alboussière [8].

In contrast to the substantial number of studies on liquid metal MHD flows in annular ducts, it appears that just a few works have been published for the case of electrolytes. Unlike liquid metal MHD flows, the Hartmann number in electrolytic flows is usually very small. Digilov [13] analyzed the flow of electrolyte driven by an azimuthal Lorentz force in an annular configuration. The author obtained an analytic solution for the case of infinite cylinders assuming that the electric field established between the cylinders (electrodes) was decoupled from the fluid flow. He performed very simple demonstrative experiments finding a pure azimuthal stable flow that showed reasonable agreement with theory. Interestingly, Digilov drew attention to the possible existence of flow regions, where, according to the theory of Marcus [14], cyclonic and anticyclonic vortices could appear, but he did not observe them. In a recent paper, Qin and Bau [15] performed a theoretical analysis of the electromagnetically driven flow of a binary electrolyte in a concentric annulus under a uniform axial magnetic field. They studied the linear stability of a pure azimuthal flow when the cylinders were infinitely long and found that when the current was directed outwards, electrochemical effects destabilized the flow, giving rise to convective flows in the transverse plane. In turn, when the current was directed inwards, electro-chemical reactions had a stabilizing effect and the azimuthal flow was linearly stable. When the annular duct has a finite height, the authors conclude that pure azimuthal flows are not possible and the flow is always three-dimensional independently on the direction of the current. In that case, the instability plays a relatively minor role in modifying the flow field.

In the present study, we investigate experimentally a free surface flow driven by an azimuthal Lorentz force in a layer of an electrolyte contained in two open cylindrical configurations. In both cases, experiments have shown a appearance of flow instability consisting of a varying number of inner cyclonic and outer anticyclonic travelling vortices for the given flow conditions characterized by the applied electric current between the electrodes and the height of the fluid layer. It is found that the instabilty appears independently of the direction of the applied radial current. Although optical methods are not of common use in MHD, we take advantage of the transparency of the electrolyte to explore through Particle Image Velocimetry (PIV) the mechanisms that trigger the instability in this electromagnetically driven flow.

1. Experimental setup and procedure. The experimental setup consists of a cylindrical open cavity of 76 mm in diameter and 12 mm in depth made of plexiglass, with one electrode made from a thin sheet of copper wrapped around the inner wall of the cavity. Another electrode is introduced in two different configurations (see Fig. 1). In the first one (configuration I), an inner concentric copper cylinder of 24.4 mm in diameter is inserted so that the fluid is contained in the gap between the cylinders. In the second configuration, a circular coin-shaped copper electrode (of the same diameter as the inner cylinder of configuration I) is placed concentrically and embedded in the bottom of the container so that the fluid occupies the whole extension of the cylindrical container. The gap between the electrodes is L=25.8 mm. In both configurations, the container is filled with a weak electrolytic solution of sodium bicarbonate ($NaHCO_3$) at 8.6% by weight forming a layer, whose thickness h is varied from 2.5 mm to 10 mm. The container is placed on top of a rectangular ferrite permanent magnet (150 mm × 100 mm× 25.4 mm) so that an approximately uniform magnetic field in the direction of the axis of the cylinder exists within the layer thickness. The magnetic field strength at the bottom of the container is $B_0 = 0.04$ T. When an electric potential difference is set between the electrodes, a DC radial electric current, whose intensity I_0 varies from 25 to 400 mA, passes (either outwards or inwards, depending on the polarity of the electrodes) through the conducting fluid. The interaction of the radial current and axial magnetic field produces a Lorentz force that generates fluid motion mainly in the azimuthal direction. The fluid rotation was clockwise for outwardly applied currents and anticlockwise for inwardly applied currents. The latter produced a stronger electrolysis that generated a large amount of bubbles. Note that the electric current in the central electrode region in configuration II was not strictly radial but mainly axial, therefore, the strength of the driving Lorentz force in that region was substantially reduced.

Fig. 2 shows a picture of the experimental setup with configuration I. The experimental procedure consisted in fixing the fluid layer thickness and then exploring the flow with a given DC current. The analyzed layer thicknesses were 2.5, 5.0, 7.5 and 10 mm and the current was varied in steps of 25 mA until the instability appeared. Results were obtained both through visualization of flow patterns using dye and through PIV. Experiments with dye were performed starting with

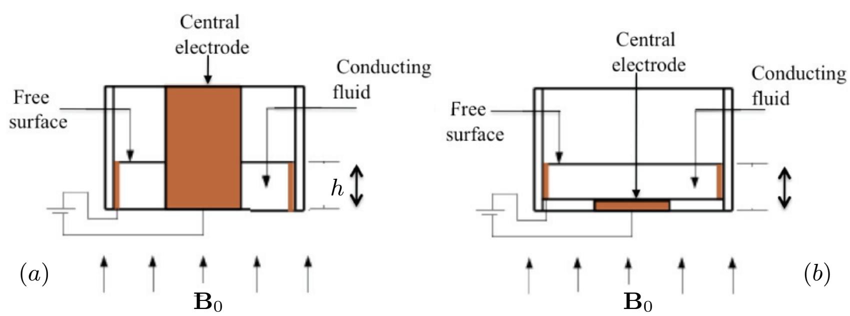

Fig. 1. Sketch of the experimental setups. (a) Configuration I with a coaxial central cylindrical electrode. (b) Configuration II with a coin-shaped central electrode embedded in the bottom wall.

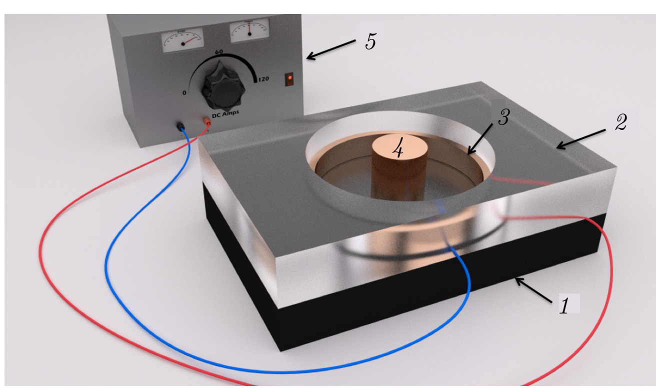

Fig. 2. The experimental setup with configuration I. *1* – ferrite rectangular permanent magnet; *2* – Plexiglass container; *3* – outer electrode; *4* – inner electrode; *5* – power supply.

the fluid at rest, with a small blob of dye on the free surface, and then setting the applied current to a fixed value. In this way, the elongation of the blob of dye caused by the Lorentz force revealed the development of the flow pattern and the eventual appearance of vortices. The flows were recorded with a Sony Handycam videorecorder (model HDR-XR100) with a resolution of 1080×720 pixels and 30 fps placed above the experimental setup. The analysis of the recorded flow patterns identified the onset of instability and the number of vortices that appeared for the given conditions. PIV measurements started also with the fluid at rest and were performed with uniform illumination from a set of three LED lamps placed on top of the plexiglass container around the cavity with the liquid. Illumination with a laser sheet was not possible due to restrictions of the experimental setup. Since the analyzed flows were relatively slow (of the order of centimeters per second), the previously mentioned videorecorder was also used for PIV analysis. Glass spheres of $10\,\mu$m in diameter covered with silver were used as tracers. In order to guarantee that the analyzed plane of flow corresponds mainly to the free surface, PIV measurements were made using only previously selected tracers. First, the tracers were centrifugated and only those that remained on the free surface were selected. Data were analyzed using the software PIV-Lab, which is a tool of MatLab.

2. Dye visualization results. In both configurations, dye visualization experiments showed the appearance of an instability in the electrolytic flow that led to the formation of anticyclonic vortices (*i.e* vortices that rotate in opposite direction to the global azimuthal flow), independently of the direction of the current. Travelling anticyclonic vortices were observed to appeared close to the wall of the outer cylindrical electrode, their number varying from four to 11 according to the flow conditions. The vortices were approximately equidistant from each other and once they appeared, remained for long times. Fig. 3 shows a sample of the visu-

(*a*)

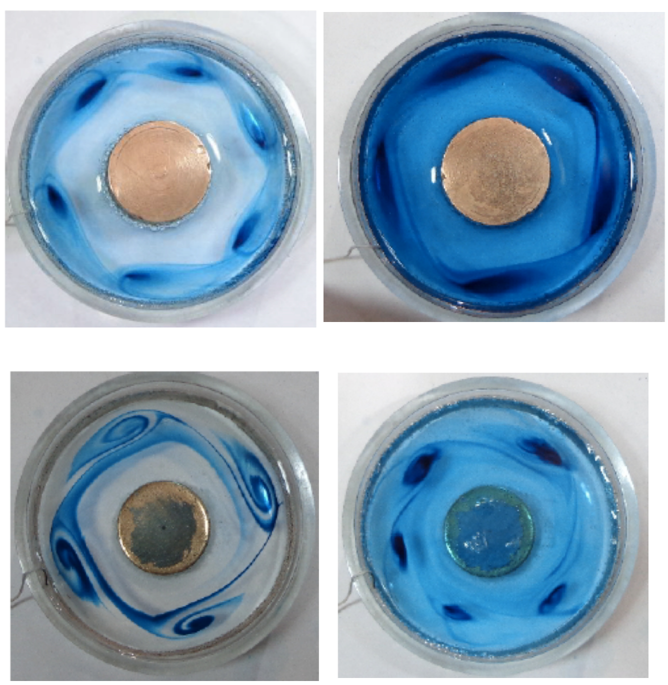

(*b*)

(*c*)

(*d*)

Fig. 3. Dye visualization of the instability observed for a layer thickness of 10 mm. (*a*) and (*b*) correspond to configuration I. (*c*) and (*d*) correspond to configuration II. The current intensity for (*a*) and (*c*) is 100 mA, and for (*b*) and (*d*) is 300 mA.

Table 1. Experimental results for configuration I.

h [mm]	h/L	I_0 [mA]	$I_0/I_{\max}$	No. of outer vortices
10	0.39	25 – 50	0.062 – 0.125	0
10	0.39	75 – 100	0.187 – 0.250	5
10	0.39	125 – 400	0.312 – 1.0	6
7.5	0.29	25 - 50	0.062 - 0.125	0
7.5	0.29	75 – 100	0.187 – 0.250	5, 6
7.5	0.29	125 – 400	0.312 – 1.0	5, 6, 7
5.0	0.19	25 – 180	0.062 – 0.450	0
5.0	0.19	190 – 400	0.475 – 1.0	8, 10, 11
2.5	0.10	25 – 250	0.062 – 0.625	0
2.5	0.10	275 – 400	0.6875 – 1.0	11

alized vortices created by the instability in both configurations. Dye visualization experiments did not reveal the existence of internal vortices close to the inner electrode. Due to the small electrical conductivity of the electrolyte ($\sigma = 6.36\,\mathrm{S{\cdot}m^{-1}}$) and the weak applied magnetic field, the Hartmann number was very low, namely, $\mathrm{Ha} = B_0 L\sqrt{\sigma/\rho\nu} \approx 0.09$, where $\rho = 1.09\cdot 10^3\,\mathrm{Kg/m^3}$ and $\nu = 10^{-6}\,\mathrm{m^2/s}$ are the mass density and the kinematic viscosity of the electrolyte, respectively. Therefore, as it occurs with weak electrolytes, the induced currents and the electromagnetic braking of the flow are negligible. Experimentally, the flow stability was controlled by varying the thickness of the fluid layer h and the applied electric current I_0. In dimensionless terms, two governing parameters were defined, namely, the aspect ratio h/L, that is, the ratio of the layer thickness to the space between the outer and inner electrodes, and the applied current parameter $I_0/I_{\max}$, where $I_{\max}$ is the maximum applied current (400 mA). From the variation of these quantities, it is possible to find the critical parameters for the occurrence of the instability. In what follows, we focuses on the results for configuration I, but similar results were found for the other configuration.

All the experiments correspond to small aspect ratios $0.01 \lesssim h/L < 0.4$. For the smallest value, the bottom friction inhibits the instability in a larger range of the applied current, where a pure azimuthal flow was observed. In fact, the smaller the layer thickness, the larger the current intensity required for the onset of the instability. As the aspect ratio increases, the current intensity required for the emergence of vortices diminishes. These observations are sumarized in Table 1, where the number of vortices originated by the instability in configuration I is presented for different experimental conditions. The map of qualitative behavior for configuration I presented in Fig. 4 identifies the region, where outer anticyclonic vortices are formed for the given values of the aspect ratio and applied current parameter.

3. Shearing zonal flow. According to Marcus [14], vortices embedded in a shearing zonal flow, where shear stress and vorticity have opposite signs, tend to be fragmented and destroyed in a turn-around time. In the regions where the signs are the same, vortices redistribute their vorticity so that its maximum value is at the center and flow structures can prevail for long times. Following Digilov [13], the criterion established by Marcus can be explored in a simplified way using an analytical solution for the azimuthal velocity that corresponds to the viscous flow of a conducting fluid between perfectly conducting infinite cylinders with an imposed potential difference under an axial uniform magnetic field (see,

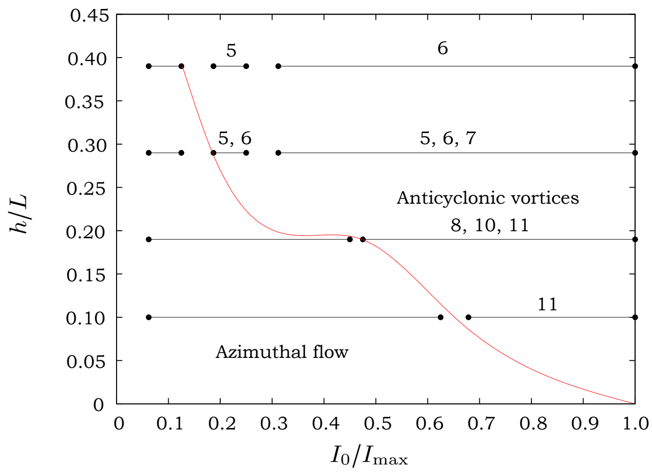

Fig. 4. Experimental map of qualitative behavior for configuration I. The curved line marks the threshold, where external anticyclonic vortices are formed for the given values of the aspect ratio (h/L) and the applied current parameter ($I_0/I_{\max}$). Numbers on top of the intervals indicate the number of vortices for the corresponding conditions.

e.g., [11, 13]). In dimensionless terms, it is possible to express this velocity profile so that it is proportional to Ha^2. For a positive (outwardly applied) current, the solution can be expressed as

$$\hat{U}_\theta(r) = \frac{\mathrm{Ha}^2}{2}\Bigg\{\ln(r+\alpha)^{(r+\alpha)} + \frac{r+\alpha}{2\alpha+1}\left[\ln\frac{\alpha^{\alpha^2}}{(1+\alpha)^{(\alpha+1)^2}} + \frac{\alpha^2(\alpha+1)^2}{(\alpha+r)^2}\ln\frac{\alpha+1}{\alpha}\right]\Bigg\}, \tag{1}$$

where the dimensionless rescaled radial coordinate is defined as $r = (r' - R_i)/L$, $\hat{U}_\theta$ is normalized by $\Delta\phi/B_0 L$, and $\alpha = R_i/L$. Here, r' is the dimensional radial coordinate and R_i is the radius of the inner cylinder. The shear stress and the vorticity, respectively, calculated from the analytical solution (Eq. (1)), take the form

$$\hat{\tau}_{r\theta}(r) = \left(\frac{\partial\hat{U}_\theta}{\partial r} - \frac{\hat{U}_\theta}{\alpha+r}\right) = \mathrm{Ha}^2\left\{\frac{1}{2} - \frac{\alpha^2(\alpha+1)^2}{(\alpha+r)^2(2\alpha+1)}\ln\left[\frac{(\alpha+1)}{\alpha}\right]\right\}, \tag{2}$$

$$\hat{\omega}_z(r) = \left(\frac{\partial\hat{U}_\theta}{\partial r} + \frac{\hat{U}_\theta}{\alpha+r}\right) = \mathrm{Ha}^2\left\{\frac{1}{2} + \ln(\alpha+r) + \frac{1}{(2\alpha+1)}\ln\frac{\alpha^{\alpha^2}}{(\alpha+1)^{(\alpha+1)^2}}\right\}. \tag{3}$$

In Fig. 5, the shear stress and vorticity (normalized by Ha^2) calculated from Eqs. (2) and (3) are plotted as a function of the rescaled radial coordinate r, using the value α=0.47 that corresponds to the experimental setup (configuration I). It is observed that $\hat{\tau}_{r\theta}$ and $\hat{\omega}_z$ have the same sign in regions close to the inner and outer cylinders, where, according to Marcus, vortices can exist. In turn, in the central shaded region, where the shear stress and vorticity have opposite signs, vortices cannot prevail. Note that according to the Marcus criterion applied to this solution, the zone, where cyclonic and anti-cyclonic vortices can dominate, depends only on the parameter α. Although these conclusions are drawn from an idealized analysis, it is interesting to explore the possible existence of inner

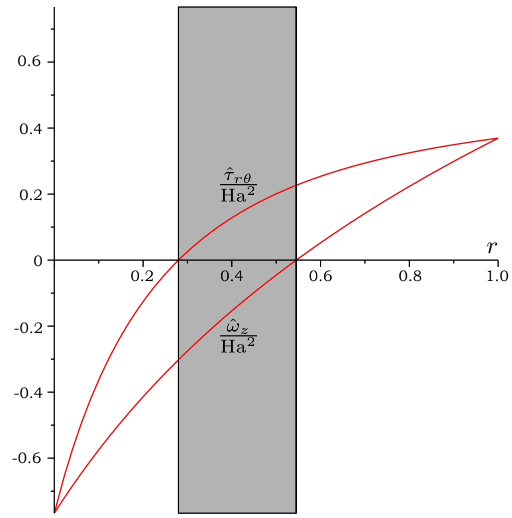

Fig. 5. Shear stress (upper curve) and vorticity (lower curve) calculated from the analytical solutions Eqs. (2) and (3) as a function of the rescaled radial coordiante r. The experimental value $\alpha = 0.47$ was used. In the shaded region, $\hat{\tau}_{r\theta}$ and $\hat{\omega}_z$ have oposite signs and, according to Marcus [14], vortices cannot prevail.

vortices not observed from the dye visualization experiments. With this purpose, a PIV analysis was performed.

4. PIV results. Consistent with the qualitative visualization, the PIV analysis revealed that an almost pure azimuthal flow occurred in those cases, where the instability did not develop, corresponding to the lower explored current intensities for a given aspect ratio (see Table 1). On the other hand, if the flow starts from rest under conditions where the instability takes place, counterflow layers develop at very early stages, close to the inner and outer cylindrical electrodes. In these layers, the flow direction is opposite to the azimuthal Lorentz force. This is observed in Fig. 6, where the velocity field obtained from PIV is shown 5.6 seconds after the flow started from rest for h=10 mm and I_0=200 mA, that is, h/L=0.39 and $I_0/I_{\max}$=0.5. In this case, the Reynolds number $\mathrm{Re} = U_{\max}L/\nu$, based on the maximum experimental velocity $U_{\max}$ obtained from PIV, takes the value Re = 704. The colors in this figure denote the vorticity. It appears that counterflow layers play the role of *side layers* in high Hartmann number duct flows, which are attached to walls parallel to the applied magnetic field. Note, however, that the counterflow layers do not have a uniform thickness, in particular, close to the inner cylinder. In Fig. 7, the azimuthal and radial velocity components obtained from the PIV measurements are plotted as functions of the rescaled radial coordinate for different times, with h=7.5 mm and I_0=150 mA (h/L=0.29, $I_0/I_{\max}$=0.375, and Re = 1160). Both components show a strong time dependence, with the azimuthal component being an order of magnitude larger than the radial component. Note that in the displayed time interval, u_θ is initially larger and counterflow layers are absent. As time proceeds, u_θ decreases and counterflow layers appear, more markedly close to the outer cylinder. In turn, in a smaller time interval, the radial component goes from negative to positive values, passing through an intermediate profile. Due to the existence of counterflow layers, it is clear that a strong shear is created at the interfaces of these layers and the core flow. Although initially no vortices were observed, eventually shear layers destabilized and gave rise to the ap-

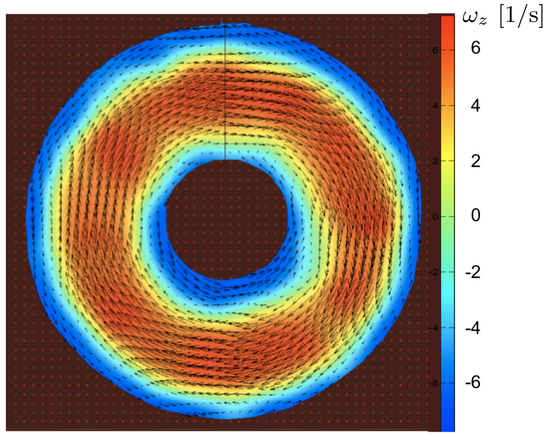

Fig. 6. The velocity field obtained from PIV in configuration I, 5.6 seconds after the flow started from rest. In the central yellow-red region, the flow is clockwise, whereas in the blue regions close to the inner and outer cylinders the flow is counterclockwise. $h = 10\,\mathrm{mm}$ and $I_0 = 200\,\mathrm{mA}$ ($h/L = 0.39$ and $I_0/I_{\max} = 0.5$). The Reynolds number based on the maximum experimental velocity is Re = 704. Colors denote the magnitude of vorticity.

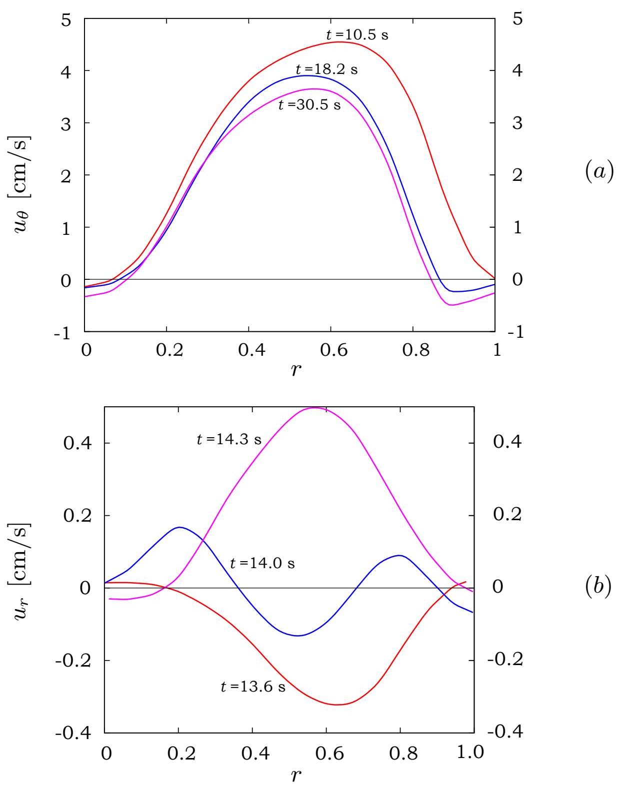

Fig. 7. Azimuthal (a) and radial (b) velocity components as a function of the rescaled radial coordiante at different times. Results were obtained from PIV measurements in configuration I with the fluid layer thickness $h = 7.5\,\mathrm{mm}$ and the current intensity $I_0 = 150\,\mathrm{mA}$ ($h/L = 0.29$and $I_0/I_{\max} = 0.375$). The Reynolds number based on the maximum experimental velocity is Re = 1160.

(*a*)

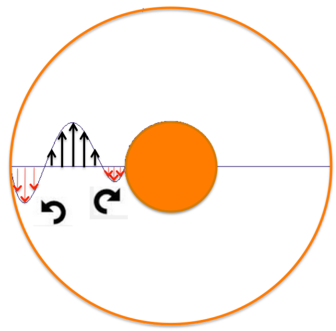

(*b*)

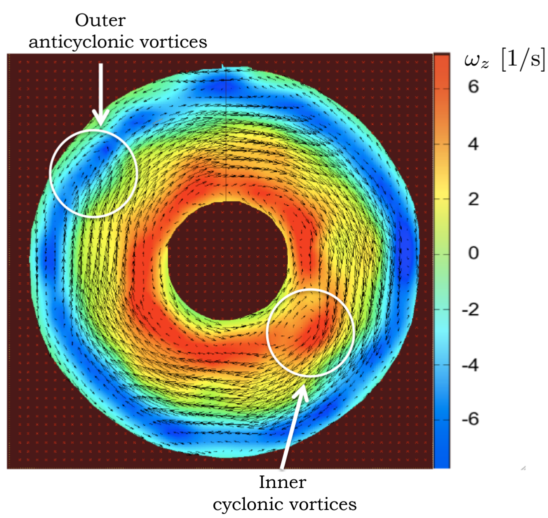

Fig. 8. (*a*) Sketch of the counterflow layers interacting with the core flow to create shear layers that originate the instability. (*b*) PIV velocity flow 14.2 seconds after the flow started from rest, where the simultaneous existence of outer anticyclonic vortices and inner cyclonic vortices is observed for $h = 10\,\mathrm{mm}$ and $I_0 = 200\,\mathrm{mA}$ ($h/L = 0.39$ and $I_0/I_{\max} = 0.5$). The Reynolds number based on the maximum experimental velocity is $\mathrm{Re} = 1194$. Colors denote the magnitude of vorticity.

pearance of vortices. Fig. 8*a* shows a sketch, which illustrates how the interaction of the counterflow layers and the core flow originates an instability that leads to the formation of outer anticyclonic vortices and inner cyclonic vortices. In Fig. 8*b*, the velocity field from the PIV measurements with h=7.5 mm and I_0=200 mA (h/L=0.29, $I_0/I_{\max}$=0.5, Re = 1194) 14.2 seconds after the flow started from rest confirms the simultaneous existence of inner and outer vortices.

5. Conclusion. We report the existence of an instability in an electrolyte flow driven by an azimutal Lorentz force in a cylindrical electromagnetic stirrer with a radially applied current under an approximately uniform axial magnetic field. The instability is characterized by the emergence of a varying number of anticyclonic travelling vortices in a plane normal to the magnetic field close to the outer electrode, which were observed through dye visualization experiments. The instability develops independently of the direction of the radial current and is governed by the aspect ratio h/L and the applied current parameter $I_0/I_{\max}$. From the experimental results, a map of qualitative behavior was built, in which the region where outer anticyclonic vortices were formed for the given values of h/L and $I_0/I_{\max}$, was identified. The PIV analysis has revealed the existence of counterflow layers close to the inner and outer electrodes. The interaction of these layers with the core flow seems to trigger the instability and originate not only outer anticyclonic vortices, but also cyclonic vortices close to the inner electrode. The existence of inner and outer vortices is consistent with the theoretical analysis of Marcus [14] for a shearing zonal flow, applied to the idealized flow between infinite cylinders. Although Digilov [13] drew attention to the possible existence of inner and outer vortices according to the Marcus criterion, he did not observe vortices in his experiment. Our results show that these vortices do exist and, for this case, the Marcus criterion is valid. As it occurs with side layers in high Hartmann number duct flows [11, 12], layers attached to the lateral conducting walls play an active role in the flow evolution and largely determine its stability properties.

Acknowledgments. Financial support from CONACYT, Mexico, through project No. 240785 is acknowledged. J. Pérez-Barrera and J.E. Pérez-Espinoza acknowledge grants from CONACYT. A. Ortiz acknowledges a postdoctoral grant from DGAPA-UNAM.

REFERENCES

[1] C.C. Chang and T.S. Lundgren. Flow of an incompressible fluid in a hydrodynamic capacitor. *Phys. Fluids.*, vol. 2 (1959), no. 6, pp. 627–632.

[2] K.O. Kessey. Rotating electrically conducting fluid in a long cylinder. *AIAA Journal*, vol. 2 (1964), no. 5, pp. 864–871.

[3] S. Schweitzer and A. Soler. One-dimensional viscous mangetofluiddynamic flow in an annulus. *J. Franklin Inst.*, vol. 289 (1970), no. 6, pp. 445–456.

[4] J.A. Baylis. Experiments on laminar flows in curved ducts of square cross-section. *J. Fluid Mech.*, vol. 48 (1971), pp. 417–422.

[5] J.A. Baylis and J.C.R. Hunt. MHD flow in an annular channel: theory and experiment. *J. Fluid Mech.*, vol. 48 (1971), pp. 423–428.

[6] A.A. Klyukin, Yu.B. Kolesnikov and H. Kalis. MHD instabilities and turbulence in liquid metal shear flows. In: *Liquid Metal Magnetohydrodynamics* (Eds.J. Lielpeteris and R. Moreau, Kluwer Acadademic Publisher, Dordrecht, 1989), pp. 449–454.

[7] A.A. Klyukin and A. Thess. The investigation of the turbulence origination in an electrically driven MHD flow. *Magnetohydrodynamics*, vol. 29 (1993), no. 4, pp. 341–344.

[8] P. Moresco and T. Alboussière. Experimental study of the instability of the Hartmann layer. *J. Fluid Mech.*, vol. 504 (2004), pp. 167–181.

[9] B. Mikahailovich. Some properties of turbulent rotating MHD flows under crossed electrical and magnetic fields. *Magnetohydrodynamics*, vol. 46 (2010), no. 4, pp. 381–386.

[10] B. Mikahailovich, A. Shapiro, S. Sukoriansky, and I. Zilberman. Experiments with turbulent rotating MHD flows in an annular gap. *Magnetohydrodynamics*, vol. 48 (2012), no. 1, pp. 43–50.

[11] Y. Zhao, O. Zikanov, and D. Kraznov. Instability of magnetohydrodynamic flow in an annular channel at high Hartmann number. *Phys. Fluids*, vol. 23 (2011), p. 084103.

[12] Y. Zhao and O. Zikanov. Instabilities and turbulence in magnetohydrodynamics flow in a toroidal duct prior to transition in Hartmann layers. *J. Fluid Mech.*, vol. 692 (2012), pp. 288–316.

[13] Y. Digilov. Making a fluid rotate: Circular flow of a weakly conducting fluid induced by a Lorentz body force. *Am. J. Phys.*, vol. 75 (2007), pp. 361–367.

[14] P.S. Marcus. Vortex dynamics in a shearing zonal flow. *J. Fluid Mech.*, vol. 215 (1990), pp. 393–430.

[15] M. Qin and H.H. Bau. Magnetohydrodynamics flow of a binary electrolyte in a concentric annulus. *Phys. Fluids*, vol. 23 (2012), p. 037101.

Received 31.01.2015